Wetting layers caused by surface ionization in a near-critical binary liquid mixture

Dean Ripple, Xiao-lun Wu,* and Carl Franck
Laboratory of Atomic and Solid State Physics and Materials Science Center, Cornell University, Ithaca, New York 14853
(Received 25 May 1988)

Kayser [Phys. Rev. Lett. **56**, 1831 (1986)] has proposed that surface ionization provides the long-range force responsible for the wetting layers seen in the binary liquid mixture $CS_2+CH_3NO_2$ on borosilicate glass substrates. We use scaling theory to find the equation of state for the near-critical mixtures, and then derive a free-energy functional for the wetting layer that incorporates surface ionization forces. This model includes critical adsorption effects and is well suited for calculations of wetting layers in the single-phase region. Within the uncertainties of the material properties, reflectivities of the glass-liquid interface derived from the theoretical concentration profiles do agree with experimental reflectivity values for wetting layers in the one-phase region. We confirm that surface ionization produces the dominant long-range force in $CS_2+CH_3NO_2$ on glass.

I. INTRODUCTION

Binary fluid mixtures near a critical point have universal bulk properties, independent of the exact form of the long-range intermolecular forces.[1,2] In contrast, recent theoretical and experimental work suggests that long-range forces strongly affect wetting properties of the liquid mixture at a solid-liquid interface.[3,4] A quantitative understanding of the long-range liquid-liquid and solid-liquid forces is necessary both for a more stringent comparison of experimental results and theory, and for more carefully controlled and characterized experiments.

The wetting properties of carbon disulfide, CS_2, and nitromethane, CH_3NO_2, on glass are now well documented, but the long-range forces responsible for the thick nitromethane-rich wetting layers have not been conclusively identified.[5,6]

We have measured wetting-layer reflectivities for regularly stirred and randomly stirred mixtures at coexistence, and for mixtures in the single-phase region,[5,6] but because of a variety of experimental difficulties only the single-phase region data provide an adequate test of the nature of the long-range forces. Very small amounts of ionized impurities can screen out both zero-frequency dipole forces and surface ionization forces on length scales of less than 100 nm, drastically altering the wetting-layer thickness. For regularly stirred binary fluids, the narrow frequency range in which the hydrodynamics is well understood severely limits the usefulness of data,[6,7] and in the random stirring case, the effect of stirring on the wetting layers is not clear at all.

In the single-phase region data, though, wetting-layer thicknesses vary smoothly from 0 up to ≈ 60 nm close to coexistence, and any effects of ion screening should be much easier to identify than at coexistence. The short equilibration time of <1 min also does not limit the amount of data.

For these reasons we concentrate in this paper on the single phase region data, in particular data taken along trajectory A, which is illustrated in Fig. 1. Previous analysis of reflectivities along this trajectory[5] gave evidence of a retarded dispersion force producing the wetting layer, in apparent contradiction to calculations by Kayser[8] indicating that dispersion forces do not favor wetting by a nitromethane-rich phase. We have repeated these calculations, including the effects of an additional surface layer of damaged glass or adsorbed nitromethane. For wetting-layer thicknesses greater than about 1 nm the dispersion forces still do not favor wetting by a nitromethane-rich phase. Following the work of Langmuir,[9] Kayser[10] in a separate calculation has shown that ionization of the glass surface can produce nitromethane-rich wetting layers. Kayser's choice of surface charge leads to predicted wetting-layer thicknesses much less than the largest values observed on trajectory A, but other reasonable choices can give thicknesses comparable to the experimental values.

The past analysis of the trajectory-A data suffered from at least four problems: (i) the concentration profile was assumed to be a slab profile, (ii) only power-law forms for the interface potential were considered, (iii) the

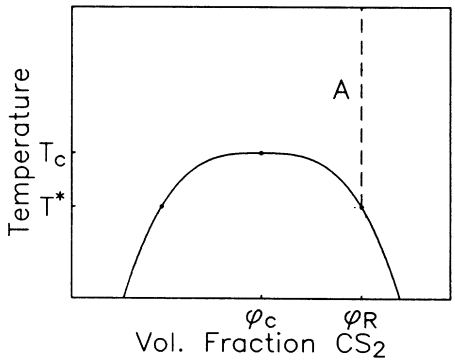

FIG. 1. Coexistence curve for the binary mixture. The data were taken along trajectory A for both increasing and decreasing temperatures. T_c is the critical temperature, T^* is the transition temperature along A ($T_c - T^* \approx 1.24$ K for the data in this paper), ϕ_c is the critical concentration, and ϕ_R is the total concentration of the sample cell.

effect of inhomogeneity of the glass substrate was neglected,[11] and (iv) the magnitude of wetting-layer thicknesses expected from the proposed physical force was not compared with the observed values.

Motivated by Kayser's initial results, we present in this paper a detailed comparison of reflectivities measured along trajectory A and reflectivities predicted by a version of the Kayser-Langmuir theory, which we modify to account for a finite correlation length and to incorporate the thermodynamics appropriate for wetting layers in the single-phase region. These modifications realistically describe any critical adsorption effects and also allow a quantitative comparison of wetting-layer thicknesses, in accordance with points (i) and (iv) above. We construct a theory in which the volume concentration of carbon disulfide, ϕ, and the electrostatic potential, ψ, are assumed to be smooth functions of the distance z from the wall. Writing the free energy as a functional of ϕ and ψ and minimizing gives us the profile $\phi(z)$. After conversion of the concentration profile into a refractive index profile $n(z)$ via the Lorentz-Lorenz relation the reflectivity of a given profile can be found and compared with the experimental values. We include in the refractive index profile a correction for inhomogeneity of the glass surface.

Plausible values of surface charge and plausible models for the solubilities of ions in the binary mixture will be shown to give theoretical reflectivity versus temperature curves in good agreement with experimental measurements. The theory predicts that the addition of bulk ions to the liquids will screen out the surface ionization forces and reduce the corresponding wetting-layer thickness. Experimental measurements on liquid mixtures with added ions agree reasonably well with this prediction. We conclude that surface ionization forces are the dominant long-range force in the system carbon disulfide and nitromethane on glass, and that these forces are calculable.

We proceed by summarizing the data and its uncertainty in Sec. II. In Sec. III, we describe the form of the free energy, including a discussion of the free energy of the bulk liquids off coexistence. To apply the results of Sec. III, we find in Sec. IV the material parameters specific to the system carbon disulfide and nitromethane. Data and theory are compared in Sec. V, and we state our conclusions in Sec. VI.

II. EXPERIMENTAL RESULTS

Previous work describes in detail the sample preparation and measurement techniques, so we only outline the most important points here.[5,6] A sealed glass and stainless steel cell holds the liquids in coexistence with the vapor phase at fixed overall volume fraction of carbon disulfide, and the cell temperature is controlled to ± 0.2 mK by immersion in a water bath. One face of a borosilicate glass prism, cleaned to give a hydroxylated surface,[12] forms the bottom face of the sample cell. The attraction of the polar nitromethane molecules to the polar hydroxyl groups provides a short-range force favoring wetting by nitromethane. All of the experiments discussed here used an overall carbon-disulfide-rich sample cell concentration, and a nitromethane-rich layer (labeled N^*) separates the glass and bulk carbon-disulfide-rich phase (labeled C^*). Measurements of the reflectivity of the glass-N^*-C^* interface provide a sensitive measure of the N^* layer thickness.

Since relating reflectivity to layer thickness requires modeling of several optical parameters, we have chosen to present our data here as the measured reflectivity. The theory curves incorporate any assumptions on optical modeling.

In Figs. 2 and 3 we present data for two sample cells (labeled cell 1 and cell 2, respectively) with $\phi = 0.733$ for the overall concentration. Because the data in Fig. 2 have much less noise at the high-temperature points, which are useful for finding the index of refraction of the bulk liquid, most of the theoretical comparisons will be made on this data.

In an attempt to screen out any electrostatic forces, we added to cell 2 1.6 mol/l of tetrabutylammonium iodide, an easily ionized salt, and the resulting reflectivity values are shown as the lowest set of symbols in Fig. 3. Conductivity measurements indicate that the salt completely dissociates in pure nitromethane at room temperature.[13] In Sec. V we discuss the theoretical curves seen in Figs. 2 and 3.

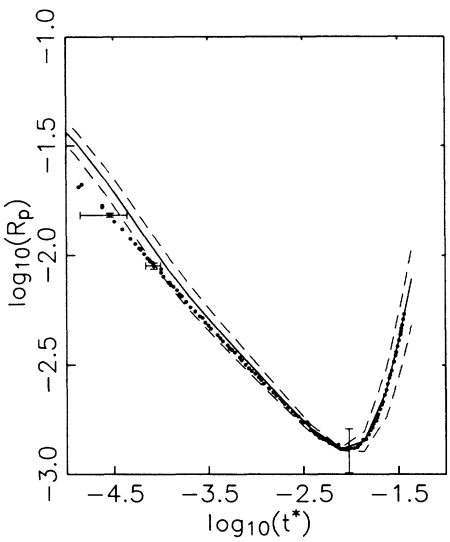

FIG. 2. Reflectivity data for cell 1 along trajectory A. This data was previously published in Ref. 5. The symbols are the measured reflectivity values, plotted with respect to the reduced temperature $t^* \equiv (T - T^*)/T^*$. To give a sense of length scales, the leftmost symbol corresponds to a wetting layer thickness of ≈ 46 nm. Horizontal error bars indicate uncertainties in $T - T^*$, and vertical error bars indicate statistical and systematic errors in the reflectivity measurement. In Sec. V we discuss the theoretical curve, which is given by the solid line. Dashed lines represent the uncertainty in the theoritical curve from errors in the optical parameters and in the free energy parameters. The angle of incidence is 1.347 rad, and the incident light is P polarized.

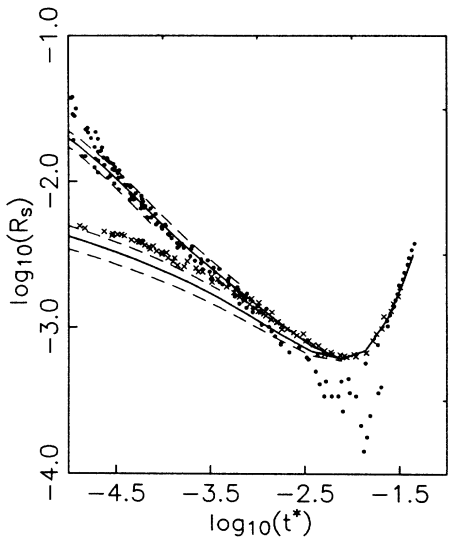

FIG. 3. Reflectivity data for cell 2 along trajectory A. The solid circles are the reflectivity values for the cell with only impurity ions, and the crosses are the reflectivity values after salt was added to the cell. We have compiled eight separate runs in this figure, and the scatter is representative of both measurement errors and reproducibility of the data. As in Fig. 2, the solid lines give theoretical curves, discussed further in Sec. V, and the dashed lines indicate the uncertainty of the theory curves. For clarity, the dashed lines are not shown for large values of t^*. The upper solid line differs from the solid line in Fig. 2 only in the optical constants obtained from the high-temperature points. For the lower solid line, we assume complete ionization of the added salt. Although we have used $\psi(0)=-0.22$ V for the lower line, the strong screening gives a reflectivity curve indistinguishable on this plot from the curve expected from critical adsorption alone. The angle of incidence is 1.265 rad, and the incident light is S polarized.

III. MODELING THE FREE ENERGY

To construct a theory for the observed wetting layers we will first assume that the system is translationally invariant in the plane of the glass surface. The concentration and electrostatic potential profiles then depend only on z, the distance from the surface. Glass surfaces have a typical surface roughness of less than 10 nm,[14] and capillary waves produce roughness in the liquid-liquid interface of roughly the same size.[15] We neglect any contributions of interface fluctuations[16] or roughness to the free energy of the wetting layer.

We work in the grand canonical ensemble, and require equilibrium between the wetting layer and a reservoir at some fixed temperature, carbon disulfide concentration, and ion concentration. We will use mks units throughout. Provided that the ion densities are low, corrections to the chemical potential from Coulomb and molecular forces can be neglected, and the number density of ion species α of charge q_α in a fluid of concentration ϕ and electric potential ψ is $\rho_\alpha(\phi)e^{-q_\alpha\psi/kT}$. In the reservoir, the ion density is $\rho_\alpha(\phi_R)$ for each species α.

We write the grand potential Ω as a functional of $\phi(z)$ and $\psi(z)$. Two terms in Ω refer to free energies of the liquid mixture alone: a gradient term $\frac{1}{2}m(\phi')^2$, and $f_e(\phi,\phi_R,t)$, the excess free energy per unit volume needed to create a volume of fluid with concentration ϕ out of a reservoir of concentration ϕ_R at reduced temperature t, where $t\equiv(T-T_c)/T_c$ and T_c is the critical temperature. The excess free energy does depend in general on the type and concentration of ions in the liquid mixture, but we assume that this effect is negligible.

To find f_e,[17] define $f_C(\phi,t)$ as the free energy per unit volume of carbon disulfide molecules when in a mixture of total concentration ϕ and temperature t. Define f_N likewise for nitromethane. With $\Delta\equiv f_C-f_N$, and assuming that there is no change in volume upon mixing the pure fluids, the Gibbs-Duhem relation gives

$$\left[\frac{\partial\Delta}{\partial\phi}\right]_t=-\frac{1}{\phi}\left[\frac{\partial f_N}{\partial\phi}\right]_t=\frac{1}{1-\phi}\left[\frac{\partial f_C}{\partial\phi}\right]_t . \tag{1}$$

The total free energy per unit volume for a given concentration can be written

$$f(\phi,t)=\phi f_C(\phi,t)+(1-\phi)f_N(\phi,t) , \tag{2}$$

and the excess free energy written in terms of f as

$$f_e(\phi,\phi_R,t)=f(\phi,t)-f(\phi_R,t)-(\phi-\phi_R)\left[\frac{\partial f(\phi_R,t)}{\partial\phi_R}\right]_t . \tag{3}$$

We define a field, $H\equiv(\Delta-\Delta_c)/\Delta_c$, and an order parameter, $M\equiv(\phi-\phi_c)/\phi_c$, where Δ_c and ϕ_c are the values of Δ and ϕ evaluated at the critical point.[2] H and M obey the scaling relation

$$H=M\,|\,M\,|^{\delta-1}h(x) , \tag{4}$$

where $x\equiv t/|\,M\,|^{1/\beta}$, and δ and β are the usual critical exponents. Reference 18 provides a useful form for the universal scaling function:

$$h(x)=E_1\left[\frac{x}{x_0}+1\right]\left[1+E_2\left[\frac{x}{x_0}+1\right]^{2\beta}\right]^{(\gamma-1)/2\beta} . \tag{5}$$

In Sec. IV we discuss the constants E_1, E_2, and x_0, but note that $x=-x_0$ defines the coexistence curve. To extend Eq. (5) into the metastable region, we set $E_2=0$ for $x<-x_0$ to satisfy the requirement that $h(x)$ and its derivative be continuous at $x=-x_0$.[19] Although more sophisticated forms[20] now exist for $h(x)$, the above form is simple to use and sufficiently accurate for our calculation. We will also neglect corrections to scaling.[1] Substitution of Eqs. (1), (2), (4), and (5) into (3) gives an expression for f_e in terms of ϕ, ϕ_R, and t.

Reference 19 discusses the gradient term in detail, including an explanation of its physical origin. We only cite the formula used to find the coefficient m:

$$m=\left[\left[\frac{\sigma}{K(\phi_{C^*}-\phi_{N^*})^2}\right]^2\frac{1}{\left|\frac{\partial\Delta}{\partial\phi}\right|}\right]_{T=T^*} \tag{6}$$

In Eq. (6), σ is the surface tension of the two coexisting liquid phases at the transition temperature T^*, ϕ_{C^*} and ϕ_{N^*} are the concentrations of the two phases, the derivative of Δ is evaluated at $\phi=\phi_{C^*}$ or ϕ_{N^*}, and K is a number depending only on the chosen form for $h(x)$. Using Eq. (9.85) from Reference 19, we find $K=0.148$ for our form for $h(x)$, in good agreement with the renormalization-group value of 0.149. Equation (6) is strictly true only at $T=T^*$, but since m diverges very weakly as $\phi\to\phi_c$ and $T\to T_c$, and since we do not discuss critical composition mixtures, we expect Eq. (6) to be a good approximation.

Noting that the integral of ion pressure over volume gives the ionic contribution to Ω, we add to the grand potential terms for the osmotic pressure and electromagnetic field pressure. We find the excess osmotic pressure by subtracting the ion pressure at $\psi=0$ from the total ion pressure,[21] and the field pressure is simply the Maxwell stress tensor.[22]

For experiments in the two phase region, f_e must be replaced by the gravitational energy of transporting N^* from the bulk meniscus down to the wetting layer.[23] Gravity will produce concentration gradients in single-phase mixtures, but along trajectory A this effect is small for $(T-T^*)/T^*\equiv t^*>10^{-7}$ and can be ignored for our experiments.[5]

Combining ionic and liquid terms, the grand potential per unit area is

$$\Omega=\int_0^\infty dz\left[\tfrac{1}{2}m(\phi')^2+f_e(\phi,\phi_R,t)-kT\sum_\alpha\rho_\alpha(\phi)(e^{-q_\alpha\psi/kT}-1)-\tfrac{1}{2}\epsilon_0\epsilon(\phi)(\psi')^2\right]. \tag{7}$$

In Eq. (7), $\epsilon(\phi)$ is the zero-frequency dielectric constant for mixtures of concentration ϕ. We will assume that all of the ions in the liquids are monovalent ($q_\alpha=\pm e$) and have solubilities described by a single $\rho(\phi)$. Under these approximations, we minimize Ω and find the equilibrium ϕ and ψ profiles by solving the Euler-Lagrange equations:

$$m\phi''-\left[\frac{\partial f_e}{\partial\phi}\right]_{t,\phi_R}+2kT\frac{d\rho}{d\phi}[\cosh(e\psi/kT)-1]+\tfrac{1}{2}\epsilon_0\frac{d\epsilon(\phi)}{d\phi}(\psi')^2=0\,, \tag{8}$$

$$\frac{d}{dz}(\epsilon\psi')=\frac{2}{\epsilon_0}\rho(\phi)\sinh(e\psi/kT)\,. \tag{9}$$

The integration of Eqs. (8) and (9) over z is truncated at a cutoff distance, d, beyond which ϕ'' is assumed negligible. By analytically integrating Eq. (9) from d to infinity, we obtain the boundary condition on $\psi(d)$,

$$\psi'(d)=2\left[\frac{\rho(\phi_R)kT}{\epsilon_0\epsilon(\phi_R)}[\cosh(e\psi/kT)-1]\right]^{1/2}. \tag{10}$$

For ϕ we require $\phi(d)=\phi_R$. A comparison of typical binding energies between nitromethane molecules and surface hydroxyl groups with the energy scale of bringing the carbon disulfide concentration to zero at the surface suggests that a plausible boundary condition at $z=0$ is $\phi(0)=0$, corresponding to pure nitromethane at the surface.[24] This approximation of a saturated surface concentration agrees with theoretical predictions for systems with strong critical adsorption.[25] The curves shown in the figures change by less than 6% in reflectivity for $t^*<10^{-2.1}$ if we use $\phi(0)=0.4$. Generally the true boundary condition for ψ at $z=0$ lies between a constant potential [$\psi(0)=\psi_0$] and a constant charge [$\psi'(0)=\psi_0'$] boundary condition.[26] We try both conditions in Sec. V.

IV. MATERIAL PARAMETERS

We first present the equations determining the constants E_1, E_2, and x_0, following the notation of Ref. 2. The quantities M and H obey the following scaling relationships:

$$\left[\frac{\partial M}{\partial H}\right]_t=\Gamma t^{-\gamma},\quad t>0$$
$$=\Gamma'(-t)^{-\gamma'},\quad t<0\,, \tag{11}$$

$$M=B(-t)^\beta,\quad t<0\,, \tag{12}$$

$$H=DM|M|^{\delta-1},\quad t=0\,. \tag{13}$$

Requiring Eq. (5) to satisfy the above equations gives $D=E_1(1+E_2)^{(\gamma-1)/2\beta}$, $x_0=B^{-1/\beta}$, and $E_2=(\beta\Gamma/\Gamma')^{2\beta/(1-\gamma)}$.

Using the amplitude ratios in Ref. 2, we find $E_2=0.30\pm0.02$, independent of any measured properties. To find E_1, we rely on two-scale-factor universality and two measured amplitudes for the system carbon disulfide and nitromethane. Reference 27 gives $B=1.36\pm0.08$ for the order parameter amplitude, and for the surface tension amplitude,[3,8] $\sigma_0=0.066\pm0.004$ J/m^2 with $\sigma=\sigma_0(-t)^{-\mu}$. We will also need to know the normalization factors for H and M, as well as T_c. From Ref. 27, $\phi_c=0.601$, and for both cells, $T_c\approx336$ K. To find Δ_c, we calculate the difference in chemical potential between carbon disulfide and nitromethane molecules in the vapor

phase at the critical temperature, assuming that at the critical point the vapors behave as an ideal gas and have vapor pressures obeying Raoult's law.[17] Tables of thermodynamic quantities of ideal gases[28] and of vapor pressure[29] give $\Delta_c=(4.26\pm0.30)\times10^8$ J/m^3, with the error determined by a conservative estimate of the error in the vapor pressure.

With our choice of H and M, the following amplitude ratios hold:[30]

$$D=\frac{R_\chi}{\Gamma B^{\delta-1}}\ , \tag{14}$$

$$\Gamma=\frac{B^2R_c\Delta_c\phi_c}{kT_c}\left[\frac{\xi_0}{R_\xi}\right]^3\ , \tag{15}$$

$$\xi_0=\frac{\Gamma\sigma_0}{4K\Delta_c\phi_cB^2}\left[\frac{\Gamma'}{\Gamma}\right]\left[\frac{\xi_0}{\xi_0'}\right]\ . \tag{16}$$

Using the values given above for K, Δ_c, ϕ_c, B, and σ_0, plus values for amplitude ratios given in Ref. 2, we find that $D=0.28\pm0.09$. The dominant errors in D are errors in B and possible errors in the application of two-scale-factor universality.[31] Our values for the equation of state amplitudes with conservative error estimates are then $E_1=0.25\pm0.08$, $E_2=0.30\pm0.02$, and $x_0=0.39\pm0.07$.

The ionic terms in the grand potential couple to the liquids via the dielectric constant, $\epsilon(\phi)$, and the solubility function, $\rho(\phi)$. To 10% accuracy we measured in a separate capacitance cell $\epsilon(\phi)=30.5-31.5\phi$ for the range $0\le\phi<0.75$ and for temperatures within a few degrees from T_c. We have no independent measurements of ionic impurities of the liquid mixtures at temperatures near the critical point, so we treat $\rho(\phi)$ as an adjustable parameter. Referring ahead to Fig. 4, the wetting layer tends to have a plateau at some concentration $\phi_{\rm WL}$. In practice only the values $\rho(\phi_R)$ and $\rho(\phi_{\rm WL})$ strongly affect wetting-layer thickness, and we can choose a convenient smooth function to interpolate between these two values. To simulate the two extremes of ions trapped strongly in the wetting layer and of ions not trapped at all, we used $\rho(\phi)=C_1\{1-\tanh[(\phi-\phi_c)/C_2]\}$ and $\rho(\phi)=$const, respectively. A choice of $C_2=0.06$ gives a smooth function for ρ while still resulting in a factor of 100 drop in ion concentration across the liquid-liquid interface. We find it convenient to use Kayser's parameter $f\equiv\rho(\phi_R)/\rho(\phi_{\rm WL})$, so that the hyperbolic tangent model for ρ has $f\approx0.01$, and the constant ρ model has $f=1$. Kayser postulated that surface charge could be scaled with liquid dielectric constant to find $\psi'(0)$ from data on water, but we do not trust this relation for two reasons. First, the surface hydroxyl groups have only partially ionic bonds,[32] reducing the effectiveness of dielectric screening relative to fully ionic bonds. Second, data on ζ potential measurements on a variety of solvents suggest that the chemical nature of the liquids, and not the dielectric constant, determine the surface charge.[33] We do not propose an alternate theory, but choose $\psi(0)$ or $\psi'(0)$ to fit the data.

To model the optical properties of the glass-liquid interface we need to know the index of refraction of the liquid mixture as a function of both concentration and temperature. Far above the transition temperature, the wetting layer contributes only slightly to the reflectivity, and the data can be used to find the bulk liquid index of refraction. We expand the index of refraction of the bulk liquid about its value at T^*: $n(t^*)=n_0-at^*$, where n_0 and a are constants obtained from a least-squares fit to the high-temperature reflectivity measurements. At a temperature of approximately $t^*=10^{-2.1}$, the bulk liquid and glass substrate have identical indices of refraction, and if the glass substrate was perfectly homogeneous and the wetting layer was negligibly thin the reflectivity would vanish at this point. The nonzero reflectivity minimum results from both a thin surface layer of damaged glass and a thin wetting layer. We include in the fit corrections for both of these contributions. As discussed in Ref. 6, we model the glass surface layer by assuming its index of refraction and fitting for the thickness of the layer. We chose to use an index of refraction of 1.442, corresponding to the value expected from measurements of void density at glass surfaces, but our results vary by less than 1% for the range of refractive index values presented in Ref. 6.

From the theoretical profiles, we can find a refractive index profile by using the Lorentz-Lorenz relation, as discussed in Appendix A, and we include this refractive index profile to account for any remaining wetting layer. To actually calculate the reflectivity from a given refractive index profile we use an optical matrix method.[34]

The fitted parameters depend slightly on the boundary conditions for ψ and the choice of $\rho(\phi)$. The range of values for all cell 1 curves in this paper are $n_0=1.5152-1.5156$, $a=0.267-0.274$, and glass surface layer thicknesses of 4.3–6.7 nm. All background fits used only those points beyond the reflectivity minimum.

Given the best fit values for the optical parameters, we use the same Lorentz-Lorenz modeling to find the reflectivity from a theoretical profile for temperatures below the point of minimum reflectivity.

V. COMPARISON OF THEORY AND EXPERIMENT

The Euler-Lagrange equations were solved numerically, as discussed in Appendix B. In Fig. 4, we show typical $\phi(z)$ profiles for several values of t^*. The inset in Fig. 4 illustrates the effect at small values of z of increasing the surface charge. As $\psi(0)$ or $\psi'(0)$ increases in magnitude, the wetting layer becomes more nitromethane-rich near the surface, which we expect from Eq. (8). Because the values of ϕ'', f_e, and ψ' are largest in the region of small z, the total free energy of the interface is dominated by the first few nm away from the wall.

The minimum in f_e for nitromethane-rich values of ϕ slowly disappears as t^* increases, and consequently the value of ϕ in the wetting layer is not as obvious in the one-phase region as on coexistence. The simplest conceivable free-energy minimization that solves for ϕ in the wetting layer would assume a slab profile for $\phi(z)$, but with the value of ϕ in the wetting layer allowed to vary. Unfortunately, for highly charged surfaces the depression of ϕ near the wall can be so strong as to give $\phi\approx0.3$ in

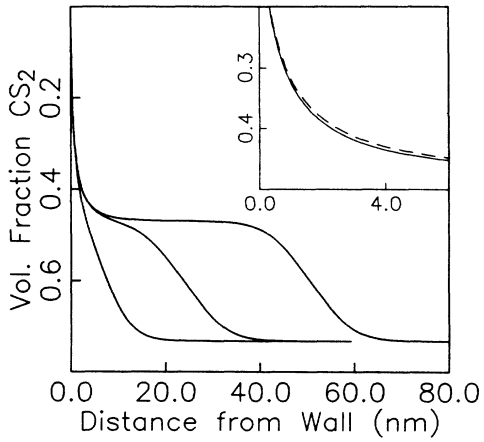

FIG. 4. Theoretical concentration profiles for several values of temperature. The main figure shows the predicted profiles for $\phi(z)$ at temperatures of $t^*=3.71\times10^{-3}$, 1.94×10^{-4}, and 2.56×10^{-5}, from left to right in the figure. For these curves, $\psi(0)=-0.22$ V and we used the $f\approx0.01$ model for the ion solubility with $C_1=0.5\times10^{-5}$ nm^{-3}. In the inset we show the effect of changes in $\psi(0)$ on the profile at small z values for $t^*=5.5\times10^{-6}$. For the solid line $\psi(0)=-0.10$ V, and for the dashed line $\psi(0)=-0.35$ V.

the wetting layer, and the corresponding rise in f_e results in wetting layer thicknesses as small as 4 nm.[35] This implausible result further motivates the more complex calculation of Sec. III.

For the sample cells in which no intentional impurities were added, the best fit to the data used the parameters $\psi(0)=-0.22$ V, and a solubility model with Debye screening length of ≈35 nm within the wetting layer and ion leakage parameter $f\approx0.01$ [hyperbolic tangent model for $\rho(\phi)$ with $C_1=0.5\times10^{-5}$ nm^{-3}]. This fit is shown as the solid line in Fig. 2 and the upper solid line in Fig. 3. The dashed lines indicate the uncertainty in the fit due to possible errors in the parameter E_1 and statistical errors in the optical parameters. Because of noise from a voltage digitizer, the lowest reflectivity values for cell 2 without added salt cannot be trusted. This problem was corrected after we added salt, so the background optical parameters for cell 2 were fitted to the reflectivity of the runs with added salt.

To predict the reflectivity when salt is added, we assumed that the salt was fully ionized and equally soluble in both the wetting layer and the bulk liquid. This gives $\rho(\phi)=10^{-3}$ nm^{-3}, resulting in a Debye screening length of 3.5 nm. Shown as the bottom solid line in Fig. 3, the theoretical curve slightly underestimates the measured reflectivities. Possible explanations for the discrepancy include incomplete ionization of the added salt, contributions to the long-range force from interface fluctuations, or shifts in the coexistence curve from the addition of the salt, with corresponding shifts in the refractive index of the wetting layer. Conductivity measurements of salt added to the binary mixture at temperatures near T_c could determine the degree of salt ionization, and for the interface fluctuations, experiments on coexistence at different temperatures could test the predicted $e^{(-z/\xi)}$ dependence of the interface fluctuation force.[16] The data do clearly indicate that the long-range force is at least partially screened by bulk ions, in qualitative agreement with the theoretical results for surface ionization forces.

Using optical constants determined from the data of cell 1, we show in Fig. 5 the effect of different surface potentials or charges. Because there is no significant difference between the curve with constant surface charge compared to the corresponding constant potential curve, we have used only the easily computed constant potential curves in the other figures. Langmuir found that beyond a characteristic length the force between two charged surfaces becomes independent of surface potential or charge. The small difference between $\psi(0)=-0.22$ V and $\psi(0)=-0.35$ V curves illustrates this effect for binary fluid wetting layers.

Figure 6 likewise shows the effect of varying the solubility model. The bottom three curves have $\rho(\phi)=$constant. In this case, only the ϕ dependence of the dielectric constant results in a repulsive long-range force between the liquid-liquid interface and the glass substrate. Confining the ions to the wetting layers adds an ion pressure to the Maxwell stress tensor, giving the top three curves in Fig. 6.

If we assume roughly 5 ionizable surface groups per nm^2,[12] the surface potential of $\psi(0)=-0.22$ V corresponds to a fractional ionization of 0.008. Any interface fluctuation force would slightly decrease the magnitude of $\psi(0)$ that gives the best fit to the data, but we cannot presently give a quantitative estimate of this decrease. No measurements of surface potential for glass surfaces immersed in nitromethane have been done, but measurements for a variety of other substrates at room tempera-

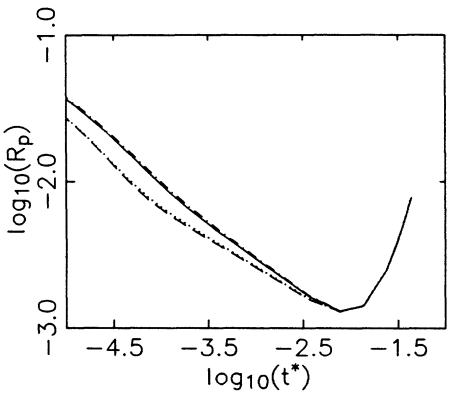

FIG. 5. Dependence of reflectivity on degree of surface ionization. All of the curves use the same parameters as in the fit for Fig. 2, but with different boundary conditions for ψ at $z=0$. Solid line, $\psi(0)=-0.22$ V; dash-dot line, $\psi(0)=-0.35$ V; dashed line, $\psi(0)=-0.10$ V. The dotted line has a constant charge boundary condition, $\psi'(0)=2.38\times10^6$ V/m chosen to agree with the $\psi(0)=-0.10$ V curve for large wetting-layer thicknesses. For larger magnitudes of $\psi(0)$, constant charge and constant potential curves are indistinguishable on the scale of the figure.

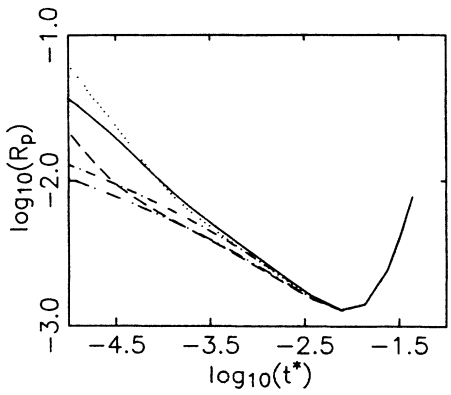

FIG. 6. Dependence of reflectivity on ion solubility. All of the curves use the same parameters as in the fit for Fig. 2, but with different ion solubility models. The bottom two curves have the solubility parameter $f=1$: $\rho(\phi)=10^{-4}$ nm^{-3} for the dash-dot-dot curve and $\rho(\phi)=10^{-6}$ nm^{-3} for the dashed curve. The top three curves use the $f=0.01$ model with different values for the parameter C_1: the dash-dot line has $C_1=0.5\times10^{-4}$ nm^{-3}, the solid line has $C_1=0.5\times10^{-5}$ nm^{-3}, and the dotted line has $C_1=0.5\times10^{-6}$ nm^{-3}.

ture give potentials of magnitude up to ≈ 0.10 V.[33] From studies of water on quartz,[36] we expect that an increase of temperature to 65 °C will increase the surface potential magnitude by roughly 0.01–0.03 V. These estimates are consistent with $\psi(0)\approx -0.10$ V. The errors indicated in Figs. 2 and 3 are comparable to the differences between the $\psi(0)=-0.10$ V and $\psi(0)=-0.22$ V reflectivity curves, so the best fit value of $\psi(0)=-0.22$ V is reasonable.

For wetting layers much thicker than both the Debye screening length and the correlation length, the critical adsorption effects become minimal and the ionic forces approach the asymptotic behavior $e^{-K_D z}$, where K_D is the reciprocal Debye screening length. In this regime calculations of wetting layer behavior can use the approximations of a slab profile for the order parameter and an exponentially decaying force on the interface.[10]

VI. CONCLUSIONS

Because the trajectory-A wetting data covers a broad range of wetting-layer thicknesses, these data provide a good test for the dependence of interface forces on the distance from the wall. Calculations of excess free energies via scaling theory further enable us to compare absolute magnitudes of measured and predicted wetting-layer thicknesses. We have shown that the combination of critical adsorption and surface ionization forces fits the data well for cells with only impurity ions. For sample cells with added ions, the theory correctly predicts a drop in wetting-layer thickness as the ions screen out the electrostatic forces. In both cases, a more stringent comparison between data and theory will require additional measurements of surface potential and ionic solubilities.

We emphasize that wetting layers resulting from critical adsorption and ionic forces do not generally depend on z as power laws.[37] The zero frequency dipole forces decay exponentially with the same screening length as the surface ionization forces, but the dipole forces have a much smaller amplitude and can be neglected. At large distances, the nonzero frequency dispersion forces must eventually exceed the exponentially decaying surface ionization forces. We calculate that for trajectory A, ionic forces balance dispersion forces at roughly 470 nm, assuming a 35 nm screening length within the wetting layer and little leakage of ions beyond the layer.[38] Dispersion forces may then be significant for the thick 400–600 nm layers observed in randomly stirred mixtures at coexistence.[5]

ACKNOWLEDGMENTS

We thank N. W. Ashcroft, D. Durian, M. E. Fisher, M. Gelfand, R. Kayser, J. Lang, and B. Widom for helpful discussions and guidance. This work was supported by the National Science Foundation, Low Temperature Physics Grant No. DMR-86-11350, and the Materials Science Center at Cornell University. One of us (D.R.) gratefully acknowledges financial support from AT&T.

APPENDIX A: MODELING THE REFRACTIVE INDEX OF THE FLUIDS

Molecular polarizability in the Lorentz-Lorenz model[8] is proportional to the function

$$g(n(\phi,t))=\frac{n(\phi,t)^2-1}{n(\phi,t)^2+2}, \tag{A1}$$

where $n(\phi,t)$ is the index of refraction at a wavelength of 632.8 nm for our experiment. For a mixture of two pure fluids, we can add the polarizabilities of each component weighted by relative volume. Including a factor M for any change in volume upon mixing, we have

$$\begin{aligned} g(n(\phi,t))&=M[\phi g(n_C)+(1-\phi)g(n_N)] \\ &\equiv MG(\phi,t)\ , \end{aligned} \tag{A2}$$

where n_N and n_C are the indices of refraction for pure nitromethane and carbon disulfide. Reference 8 gives experimental values for the refractive indices. We invert Eq. (A2) and expand about T_c to get

$$n(\phi,t)=\left.\frac{2MG(\phi,t)+1}{1-MG(\phi,t)}\right|_{t=0}+\left.\frac{\partial n(\phi,t)}{\partial t}\right|_{t=0} t\ . \tag{A3}$$

M and the derivative of $n(\phi,t)$ are assumed independent of ϕ. This assumption does not hold as $\phi\to 0$ or $\phi\to 1$, but we expect the breakdown in scaling to be an even larger error in these limits. The values of M and $\partial n(\phi,t)/\partial t$ are fixed by requiring that Eq. (A3) agree to first order in t or t^* with the experimentally measured index of refraction for the bulk liquid:

$$n(\phi_R,t)=n_0-at^* \ . \tag{A4}$$

Since we determine M through Eq. (A4) and not through a change of volume measurement, M may include quadrupole or local-field corrections to the Lorentz-Lorenz relation. Typically we find $M=0.97-0.98$, close enough to 1.0 to justify the assumption in Sec. III that there is no change in volume upon mixing.

The derivation of the Lorentz-Lorenz relation assumes an infinite, homogeneous medium, so we made numerical calculations to test its applicability to inhomogeneous interfaces. For a cubic lattice of dipoles with polarizability inhomogeneous in one dimension only, we find that beyond two lattice planes from a large discontinuity in the polarizability, the Lorentz-Lorenz relation is accurate to better than 1%. We then expect little error in applying the relation to wetting layers more than a few nanometers thick.

APPENDIX B: COMPUTATIONS

We solved the Euler-Lagrange equations as a set of finite difference equations on a discrete lattice, using the routine SOLVDE from Ref. 39. The number of lattice points was increased until a doubling of the number of points gave less than 2% change in wetting layer thickness. Typically a 400 point lattice sufficed. The finite cutoff distance contributed errors of less than 1% provided that we chose $d>l+14\xi$, where l is the wetting layer thickness and ξ is the correlation length.

The nonlinearity of the equations required a careful choice of initial values for $\phi(z)$ and $\psi(z)$. We guessed $\phi(z)$ for a small value of l and solved for $\psi(z)$ using the programs RKQC and ODEINT from Ref. 39. We then increased l in steps, solving for ψ at each step with SOLVDE until we had a set of $\psi(z)$ and $\phi(z)$ curves with which we could initialize the full set of equations.

*Current address: Exxon Research & Engineering Co., Route 22, East Clinton Township, Annandale, NJ 08801.

[1]S. C. Greer, Phys. Rev. A **14**, 1770 (1976).

[2]A. Kumar, H. R. Krishnamurthy, and E. S. R. Gopal, Phys. Rep. **98**, 57 (1983).

[3]Douglas J. Durian and Carl Franck, Phys. Rev. Lett. **59**, 555 (1987); Phys. Rev. B **36**, 7307 (1987).

[4]C. Ebner and W. F. Saam, Phys. Rev. Lett. **58**, 587 (1987).

[5]Xiao-lun Wu, Mark Schlossman, and Carl Franck, Phys. Rev. B **33**, 402 (1986).

[6]Xiao-lun Wu, Dean Ripple, and Carl Franck, Phys. Rev. A **36**, 3975 (1987).

[7]R. F. Kayser, M. R. Moldover, and J. W. Schmidt, J. Chem. Soc., Faraday Trans. 2 **82**, 1701 (1986).

[8]R. F. Kayser, Phys. Rev. B **34**, 3254 (1986).

[9]Irving Langmuir, Science **88**, 430 (1938).

[10]R. F. Kayser, Phys. Rev. Lett. **56**, 1831 (1986); J. Phys. (Paris) **49**, 149 (1988).

[11]Reference 6 discusses these effects in detail. We have observed that when the glass and bulk liquid are matched in refractive index the reflected beam is still well defined, and we conclude that surface inhomogeneity and not scattered light is responsible for the minimum reflectivity value seen in Figs. 2 and 3. In Ref. 5 this minimum reflectivity was mistakenly subtracted as background signal.

[12]Ralph K. Iler, *The Chemistry of Silica* (Wiley, New York, 1979), p. 633.

[13]A. K. R. Unni, L. Elias, and H. I. Schiff, J. Phys. Chem. **67**, 1216 (1963).

[14]K. Vedam and M. Malin, Mater. Res. Bull. **9**, 1503 (1974).

[15]R. Lipowsky, Phys. Rev. B **32**, 1731 (1985). To estimate the interface roughness we use the interface force from Ref. 10, assuming that all ions are trapped within the wetting layer and that the wetting layer profile is a slab. We find roughnesses ranging from roughly 5 nm for a 20 nm wetting layer to 7 nm for a 60 nm wetting layer.

[16]Michael E. Fisher, J. Chem. Soc., Faraday Trans. 2 **82**, 1569 (1986).

[17]J. N. Murrell and E. A. Boucher, *Properties of Liquids and Solutions* (Wiley, Chichester, 1982), Chap. 6.

[18]M. Vicentini-Missoni, J. M. H. Levelt Sengers, and M. S. Green, J. Res. Natl. Bureau Stand. **73A**, 563 (1969).

[19]J. S. Rowlinson and B. Widom, *Molecular Theory of Capillarity* (Clarendon, Oxford, 1982), Chap. 9.

[20]J. V. Sengers and J. M. H. Levelt Sengers, Ann. Rev. Phys. Chem. **37**, 189 (1986).

[21]E. M. Lifshitz and L. P. Pitaevskii, *Statistical Physics, Part 1* (Pergamon, Oxford, 1980), p. 267.

[22]L. D. Landau, E. M. Lifshitz, and L. P. Pitaevskii, *Electrodynamics of Continuous Media* (Pergamon, Oxford, 1984), p. 59.

[23]P. G. de Gennes, Rev. Mod. Phys. **57**, 827 (1985).

[24]From M. D. Joesten and L. J. Schaad, *Hydrogen Bonding* (Dekker, New York, 1974), p. 2 and Appendix, even very weak hydrogen bonds have energies of 2–10 kJ/mol. With roughly 5 binding sites per nm^2 (Ref. 12), this gives 0.02–0.1 J/m^2 for the binding energy of nitromethane. In comparison, the liquid interface energies from Eq. (7) with $\phi(0)=0$ are always less than 0.005 J/m.^{2}

[25]L. Peliti and S. Leibler, J. Phys. C **16**, 2635 (1983).

[26]Jacob N. Israelachvili, *Intermolecular and Surface Forces* (Academic, London, 1985), p. 185.

[27]E. S. R. Gopal *et al.*, Phys. Rev. Lett. **32**, 284 (1974); Ref. 1. We use the more conservative errors of Greer, and obtain the amplitude B from the first term of Greer's fit that includes corrections to scaling.

[28]J. Phys. Chem. Ref. Data **11**, Suppl. 2, 89 (1982); **11**, Suppl. 2, 90 (1982).

[29]*International Critical Tables of Numerical Data, Physics, Chemistry and Technology*, edited by E. W. Washburn (McGraw-Hill, New York, 1928), Vol. 3, pp. 23 and 28.

[30]The amplitude ratio in Eq. (16) is equivalent to Eq. (9.83) of Ref. 19.

[31]Hector Chaar, Michael R. Moldover, and James W. Schmidt, J. Chem. Phys. **85**, 418 (1986).

[32]Linus C. Pauling, *The Nature of the Chemical Bond* (Cornell University Press, Ithaca, New York, 1940), p. 71.

[33]Mohamed E. Labib and Richard Williams, J. Colloid Interface Sci. **97**, 356 (1984).

[34]Max Born and Emil Wolf, *Principles of Optics* (Pergamon, Oxford, 1980), p. 51.

[35]The exact parameters used were $\psi'(0)=2.7\times10^8$ V/m,

$\rho(\phi)=10^{-5}$ nm^{-3} in the wetting layer, and 0 beyond the wetting layer. Surface tension effects were neglected.

[36]P. Somasundaran and R. D. Kulkarni, J. Colloid Interface Sci. **45**, 591 (1973).

[37]Applications of power laws in our previous work, including Ref. 5 and Kumudini Abeysuriya, Xiao-lun Wu, and Carl Franck, Phys. Rev. B **35**, 6771 (1987) are not strictly valid, for example.

[38]We followed the calculaton of Ref. 8 and find for the pressure $P \approx H/l^4$ with $H \approx -0.7\times 10^{-3}$ J m, where a negative value for H does not favor wetting.

[39]William H. Press, Brian P. Flannery, Saul A. Teukolsky, and William T. Vetterling, *Numerical Recipes* (Cambridge Univeristy Press, Cambridge, 1986), Secs. 15.1 and 16.3.